Modeling and Managing Void Generation in Out-of-Autoclave Fast-Cure Prepregs

Elham Pakzad[1*], Malcolm Lane[2], Goran Fernlund[2,1], Anoush Poursartip[1,2],

[1] Composites Research Network, Department of Materials Engineering and Mechanical Engineering, The University of British Columbia, Vancouver, Canada

[2] Convergent Manufacturing Technologies, Vancouver, Canada

* *Elham Pakzad (elham.pakzad@composites.ubc.ca)*

Keywords: *Void generation; Porosity; Fast-cure; Prepreg; Modeling*

1. Abstract

Void generation during composite processing remains a major challenge affecting laminate quality and structural performance, particularly for fast-cure out-of-autoclave (OoA) prepregs where low processing pressure and short cure cycles increase the risk of porosity formation. To predict and control void evolution, several analytical and numerical models have been previously developed by others, based on the governing mechanisms of gas flow, resin flow and compaction, gas diffusion, and resin viscoelastic behavior.

In this study, previously developed gas–resin flow and diffusion-based models are assembled with the intention to predict void evolution and residual porosity in fast-cure OoA prepreg laminates. By combining and integrating the dominant governing mechanisms during debulk and cure, the proposed framework is intended to enable improved prediction of porosity evolution and final laminate quality under rapid OoA processing conditions. In this paper, this proposed model framework is presented alongside preliminary OoA porosity experiments using µCT characterization.

2. Introduction

Out-of-autoclave (OoA) composites manufacturing has become an attractive alternative to conventional autoclave processing because it significantly reduces manufacturing cost while enabling the production of aerospace-grade composite structures. Vacuum bag only (VBO) prepregs are specifically designed with partially impregnated fiber tows that create interconnected pathways for gas evacuation during curing [1].

Despite these advantages, void formation remains one of the primary challenges in OoA processing because low consolidation pressures limit void suppression and resin infiltration compared with autoclave processing [2]. The problem becomes more critical in fast-cure prepregs, where shortened processing times reduce the available time for air evacuation and resin redistribution.

Void evolution in prepreg laminates is governed by several coupled mechanisms, including gas flow through porous media, resin flow and compaction, gas diffusion, and resin cure shrinkage with viscoelastic effects [3]. Depending on the processing stage, porosity models may rely on a single dominant mechanism or a combination of multiple coupled mechanisms. Therefore, understanding and modeling these coupled transport phenomena are essential for predicting void evolution and optimizing OoA processing conditions to minimize residual porosity

3. Review of Existing Void/Porosity Evolution Models

Various analytical and numerical models have been proposed to describe void formation, transport, and evolution during composite debulking and curing. These models differ primarily in the physical mechanisms considered and the degree of coupling between gas transport, resin flow, gas diffusion, and resin shrinkage. The following sections discuss the most practical porosity models reported in the literature.

For a compressible gas within a porous carbon/epoxy laminate, the conservation of mass is governed by the following continuity equation [4]-[9]:

$$\frac{\partial}{\partial t}(\rho_g \varphi) + \nabla.(\rho_g v_g) = \dot{m} \tag{1}$$

where ρ_g is the gas density, φ is the porosity, v_g is the gas velocity vector, and $\dot{m}$ represents the mass source term.

Equation (1) forms the basis of many porosity prediction models. A similar continuity equation can also be used to describe the evolution of an individual spherical void [12]-[16]:

$$\frac{\partial}{\partial t}(\rho_g) + \nabla.\left(\rho_g v_g\right) = 0 \tag{2}$$

A summary of the major models and governing laws based on the primary gas and resin behaviors is presented in Figure 1.

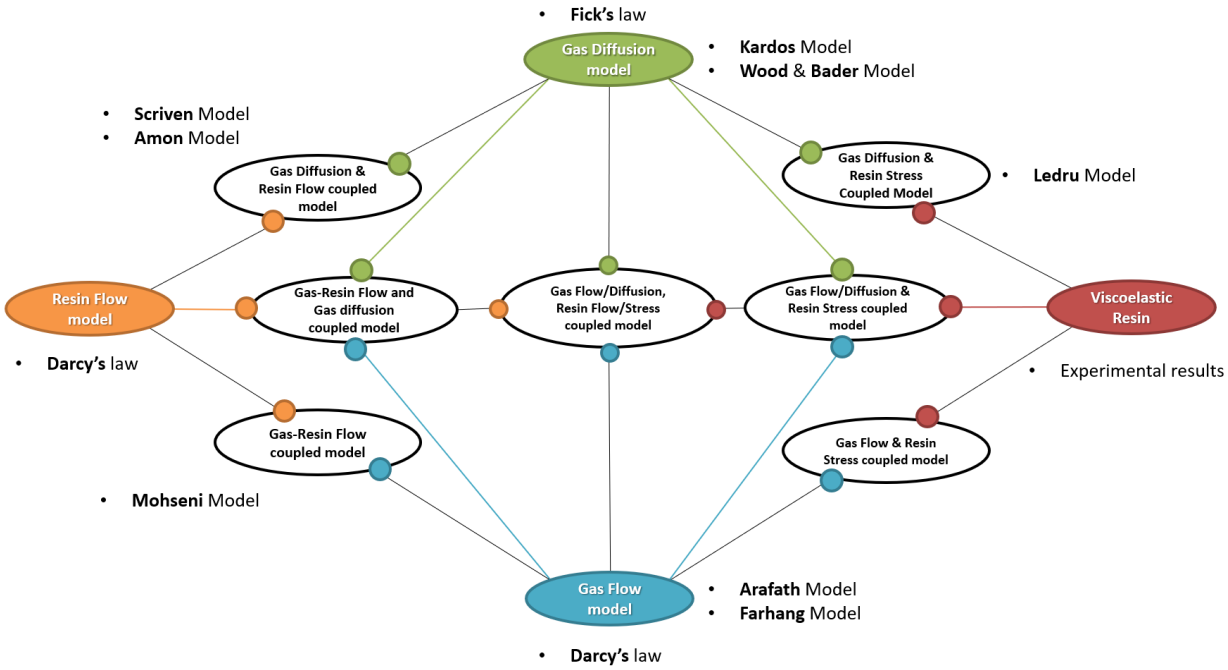

Figure 1 Schematic summary of the major porosity prediction models and governing laws based on the primary gas flow, resin flow [[4]-[6]], gas diffusion, and viscoelastic resin behaviors [13][16] involved in composite debulking and curing processes.

3.1. Gas-Flow-Based Porosity Models

When gas transport through a porous medium is assumed to be the dominant mechanism for void removal in a dried laminate with no other volatile generation mechanisms ($\dot{m} = 0$), Equation (1) can be reduced to a gas-flow-based model:

$$\varphi \frac{\partial P_g}{\partial t} + \frac{K_g}{\mu_g} . \frac{\partial}{\partial x}\left(P_g . \frac{\partial P_g}{\partial x} \right) = 0 \tag{3}$$

where φ is the porosity, p is the gas pressure, K_g is the gas permeability, and μ_g is the gas viscosity.

Based on the work of Arafath et al. [5] and Farhang et al. [6], and assuming ideal gas behavior with Darcy flow, the minimum debulking time required to achieve a target porosity can be estimated as follows [5]-[7]:

$$t^* = \frac{\mu}{p_0} \frac{\varphi}{K_g} \left[-\frac{1}{0.9} \ln\left(\frac{\varphi_F}{\varphi} \right) \right]^{\frac{1}{0.6}} L^2 \tag{4}$$

where p_0 is the initial gas pressure, φ_F is the desired final porosity, and L is the transport length in the one-dimensional gas transport model.

3.2. Resin-Flow-Based Porosity Models

If resin flow is assumed to be the dominant mechanism controlling porosity reduction in a laminate, the conservation of mass for an incompressible resin in the absence of mass generation ($\dot{m} = 0$) can be expressed as [17]:

$$\frac{\partial V_s}{\partial t} + \nabla.(V_s \overline{v_s}) = 0 \tag{5}$$

where V_s is the solid volume fraction, and $\overline{v_s}$ is the local velocity of the medium.

Assuming Darcy flow, this approach has been widely used to model tow impregnation for different fiber architectures [3], [8],[9],[17]-[23].

3.3. Coupled Gas–Resin Flow Porosity Model

To account for simultaneous gas evacuation and resin infiltration, Mohseni et al. [4] developed a coupled gas–resin flow model based on Darcy's law:

$$\varphi \frac{\partial P_g}{\partial t} + P_g \frac{\partial \varphi}{\partial t} - \frac{\partial}{\partial x}\left(\frac{K_{g,x}}{\mu_g} P_g \frac{\partial P_g}{\partial x}\right) = 0 \tag{6}$$

$$\frac{\partial \varphi}{\partial t} = -\frac{K_{r,z}}{h^2 \mu_r (1 - V_f)} \frac{P_g + P_c - P_a}{1 - \varphi} \tag{7}$$

Where $K_{r,z}$ is the transverse permeability, h is the laminate thickness, P_a is the applied pressure, and P_c is the capillary pressure.

3.4. Diffusion-Based Void Growth Models

Void growth within the resin can also be governed by diffusion of dissolved gases and moisture. Following the earlier works of Weinberg, Amon, and Scriven [10]–[12], Kardos et al. [13] developed one of the earliest diffusion-based void growth models:

$$R_{void} = 4\sqrt{D\left(\frac{C_\infty - C_{sat}}{\rho_g}\right)t} \tag{8}$$

where R_{void} is the void radius, D is the diffusion coefficient, C_∞ is the bulk gas concentration, C_{sat} the concentration at the void surface.

Using a similar approach, another widely used model for predicting void radius evolution in composite manufacturing was developed by Wood and Bader [14], and can be expressed as follows:

$$\frac{dR_{void}}{dt} = \frac{D(C_\infty - C_{sat})}{\rho_g R_{void}}\left[1 + \frac{R_{void}}{\sqrt{\pi D t}}\right] \tag{9}$$

3.5. Viscoelastic-Based Void Growth Models

After gelation, resin flow becomes negligible and internal stresses generated by cure shrinkage and thermo-mechanical constraints can influence defect formation. Mohseni et al. [15] showed that post-gelation void evolution is strongly governed by hydrostatic stresses and cure rate effects.

3.6. Coupled Viscoelastic and gas Diffusion Void Growth Model

The diffusion-based models developed by Kardos et al. [13] and Wood and Bader [14] provided the foundation for predicting void growth driven by dissolved gas diffusion. Building on these

earlier studies, Ledru et al. [16] developed a coupled viscoelastic and diffusion-based model to improve prediction of final void size under realistic curing conditions. Unlike previous simplified approaches, the model accounts for non-isothermal and non-isobaric processing conditions, gas molecular weight variation, and surface tension effects during polymerization. The resulting coupled model can be expressed as follows:

$$\frac{d}{dt}\left(\frac{M_g}{T}\left(p_{imp}R_{void}^3 + 2\gamma_{LV}R_{void}^2\right)\right) = 3R_bR_{void}D(C_\infty - C_{sat})\left[1 + \frac{R_{void}}{\sqrt{\pi Dt}}\right] \quad (10)$$

where M_g is the molecular weight of the gas within the void, p_{imp} is the externally applied hydrostatic pressure, γ_{LV} is the liquid–vapor surface tension, and R_b is the universal gas constant.

4. Coupled Modeling Framework

The gas-flow and coupled gas–resin flow models discussed in Sections 3.1 and 3.2 can successfully predict porosity evolution in prepreg laminates when no internal mass generation occurs within the material. However, during practical composite processing, absorbed moisture may generate additional gaseous species during heating and curing, significantly influencing void evolution and residual porosity.

Although diffusion-based models described in Sections 3.3 and 3.4 can predict the growth or shrinkage of individual voids due to dissolved gas and moisture transport, they are generally limited to single-void analysis and cannot predict overall laminate porosity evolution.

To overcome this limitation, a coupled modeling framework is proposed based on the conservation of mass (Equation (1)), in which gas–resin flow (Equation (6)) is coupled with diffusion-driven mass generation effects [10]–[16]. The proposed model enables simultaneous prediction of gas evacuation, resin infiltration, and diffusion-driven void evolution throughout debulking and curing.

By fitting the model to experimental results, the total porosity evolution during processing can be predicted, enabling optimization of cure-cycle parameters to achieve minimized residual porosity.

5. Experimental Procedure

5.1. Material System

The material used in this study is a unidirectional carbon fiber reinforced epoxy, with a resin content of 33.5 wt.%. Resin viscosity evolution during cure was obtained from cure kinetics and viscosity models implemented in the commercial process simulation software RAVEN.

5.2. Lay-up and Moisture Conditioning

Eight-ply laminates (3 in × 5 in) were fabricated according to the manufacturer's recommended procedures. The laminates were conditioned for five days in sealed humidity-controlled containers using saturated salt solutions in accordance with ASTM E104-20a [24]. Relative humidity levels

of 20%, 44%, 74%, and 95% were maintained using silica gel and saturated salt solutions while temperature and humidity were continuously monitored.

5.3. Debulking and Cure Cycle

Following moisture conditioning, laminates were vacuum bagged on a 3.5 mm glass tool plate covered with a non-perforated FEP release film, following the procedure described by Kay [6]. The vacuum bagging configuration is shown in Figure 2.

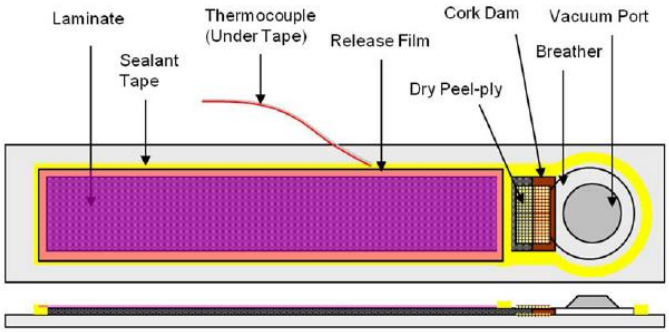

Figure 2 Vacuum bagging arrangement (nylon bag not shown for clarity) [6].

The laminates were debulked under full vacuum for 5 minutes at room temperature and subsequently cured according to the manufacturer-recommended OoA cure cycle: heating to 120 ºC at 1.5 ºC/min followed by a 180 min dwell, then heating to 180 ºC at the same rate followed by a second 180 min dwell.

To investigate porosity evolution, the cure cycle was interrupted at selected processing times (0, 30, 40, 50, 100, 190, 240, and 450 min), and samples were characterized using micro-CT analysis.

5.4. Porosity Measurement Methods

Porosity evolution and void morphology were characterized using micro-computed tomography (micro-CT) and image analysis. Samples were mounted in System Three Cold Cure Epoxy prior to scanning.

Micro-CT imaging was performed using a ZEISS Xradia 520 Versa system at 3 µm voxel resolution, 40 kV accelerating voltage, and 1601 projections. The reconstructed image stacks were analyzed using ImageJ to quantify porosity and evaluate void morphology throughout curing.

6. Results and Discussion

6.1. Void Evolution During Debulking

The total porosity was calculated from the analyzed micro-CT image stacks using ImageJ according to Equation (11). To account for orientation-dependent variations in image analysis, porosity measurements were evaluated from the 0°, 90°, and top-view directions.

$$Porosity = \frac{Sum\ of\ (Area\ \times thickness\ of\ slice)}{lenght \times width \times total\ thickness} \tag{11}$$

Figure 3 shows representative micro-CT images before and after the 5-minute debulking at room temperature, illustrating the initial evolution of void distribution and porosity. Figure 4 presents the corresponding changes in void morphology observed from the top-view orientation.

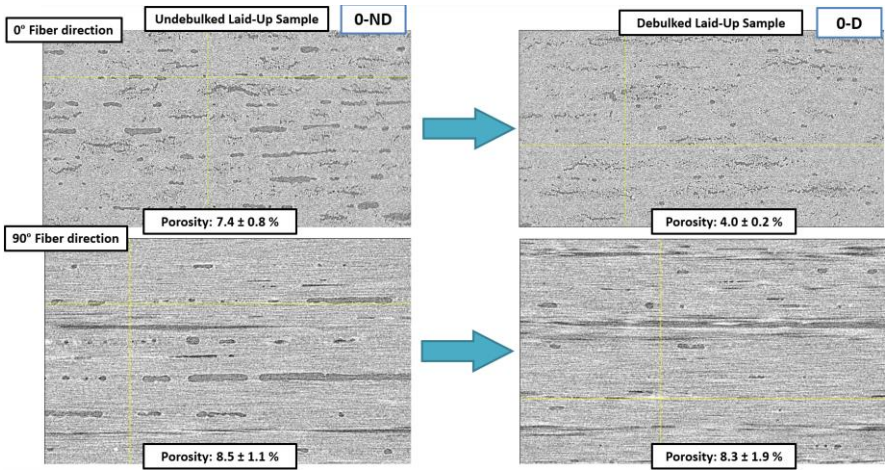

Figure 3 Representative micro-CT images of the laminate: (0-ND) before debulking and (0-D) after the 5-minute debulking procedure.

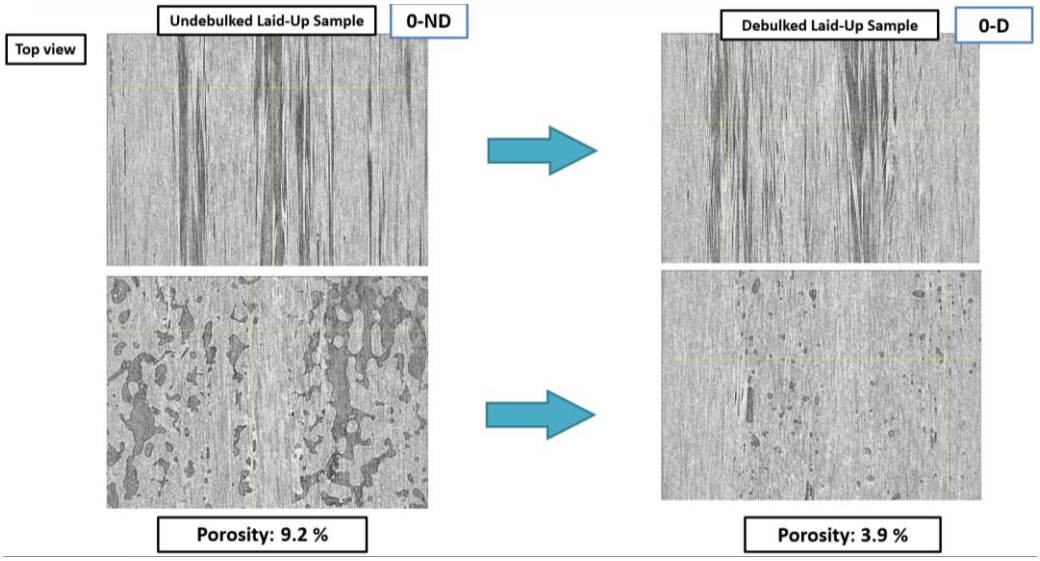

Figure 4 Variation in void morphology observed from the top-view orientation before debulking (0-ND) and after a 5-minute debulking procedure at room temperature (0-D).

6.2. Porosity Evolution During Cure

Figure 5 illustrates the porosity evolution and void morphology changes for laminates conditioned at 20% relative humidity. Voids located between fiber tows formed interconnected channels that enabled gas evacuation and resin infiltration during cure. These channels progressively disappeared as they became filled with resin, whereas isolated entrapped voids showed only minor size changes and remained within the fully cured laminate.

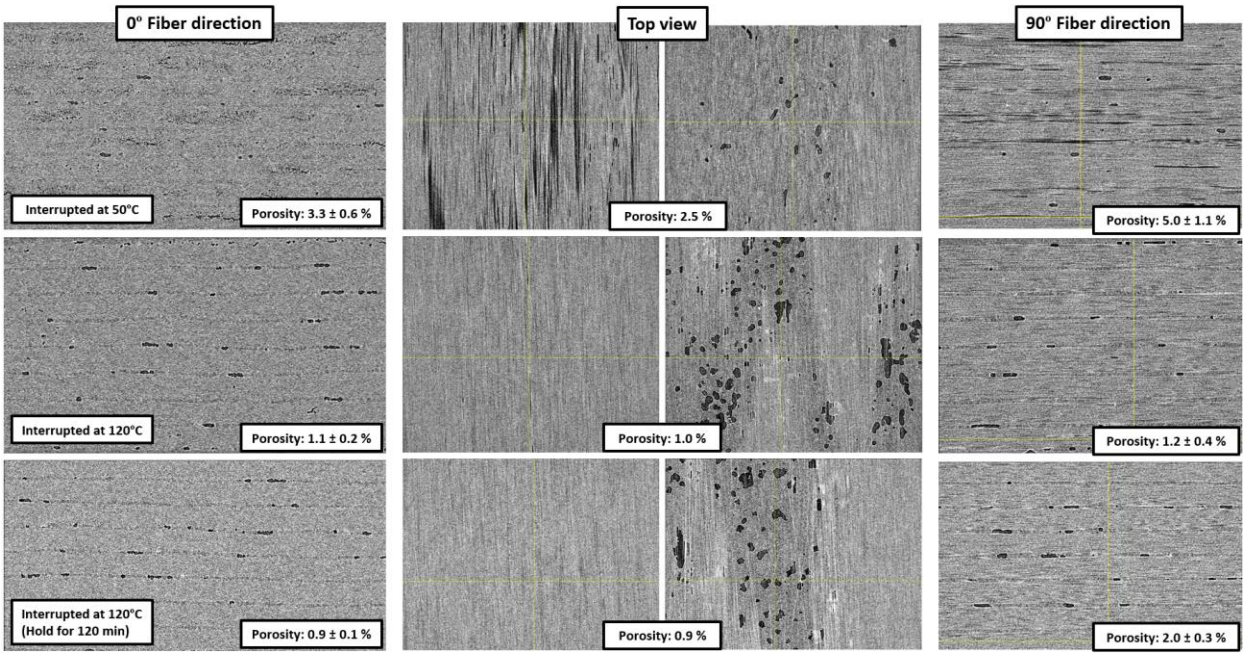

Figure 5 Porosity evolution and void morphology changes in laminates conditioned at 20% relative humidity during curing.

6.3. Effect of Moisture and Diffusion

Figure 6 presents the porosity evolution of laminates conditioned at relative humidity levels of 20% and 95%, along with the final porosity values measured for laminates conditioned at 45% and 75% relative humidity

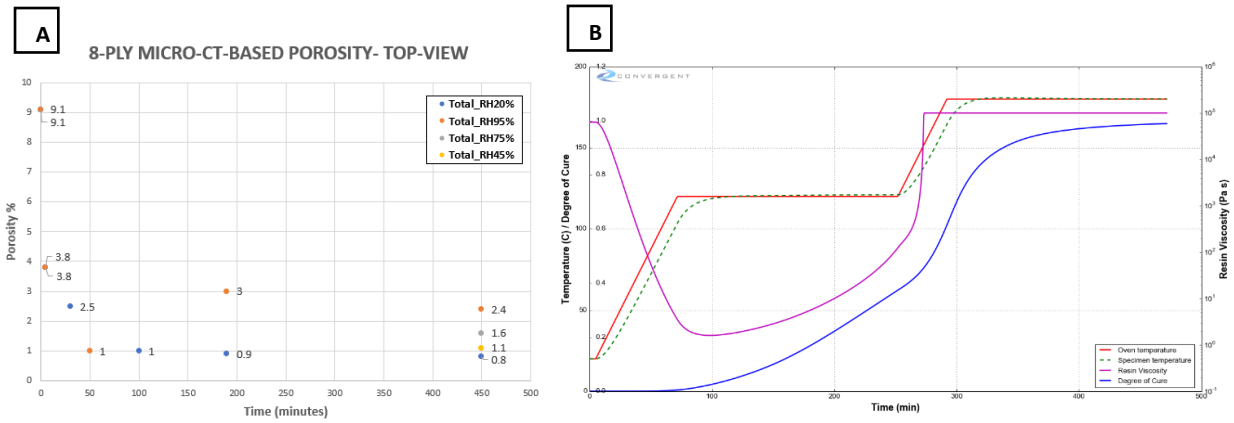

Figure 6 Porosity evolution of laminates conditioned at different relative humidity levels throughout the debulking and curing processes. (B) Applied cure cycle together with the corresponding viscosity evolution and degree of cure

7. Conclusions

This paper has presented preliminary results from an investigation into void evolution in fast-cure out-of-autoclave (OoA) prepreg laminates using a combined experimental and modeling approach. Existing porosity models based on gas flow, resin flow, diffusion, and viscoelastic effects have

been integrated into a coupled framework intended to capture the dominant mechanisms governing void evolution during debulking and curing.

Micro-CT analysis confirms that interconnected void channels between fiber tows act as primary pathways for gas evacuation and resin infiltration, while isolated entrapped voids exhibit limited evolution during cure. Moisture conditioning was also found to significantly influence porosity evolution, highlighting the importance of diffusion-driven mechanisms associated with absorbed moisture and dissolved gases.

The proposed coupled gas–resin flow and diffusion-based model promises an improved approach for predicting laminate porosity evolution and optimizing cure-cycle parameters to minimize residual porosity in aerospace composite structures.

Acknowledgements

The authors would like to acknowledge the financial support of the industrial members of the Composites Research Network (The Boeing Company, Toray CMA, and Convergent) as well as the Canadian Federal Government (NSERC and PacifiCan) as well as many useful conversations with our industrial colleagues.

8. References

[1] T. Centea, L. K. Grunenfelder, S. R. Nutt. "*A review of out-of-autoclave prepregs – Material properties, process phenomena, and manufacturing considerations"*. Composites: Part A, 132-154, 2015

[2] L. K. Grunenfelder, S. R. Nutt. "*Void formation in composite prepregs – Effect of dissolved moisture"*. Composites Science and Technology, 2304-2309, 2010

[3] L. Farhang, M. Mohseni, N. Zobeiry, G. Fernlund. "*Experimental study of void evolution in partially impregnated prepregs"*. Journal of Composite Materials, Vol. 54(11) 1511–1523, 2019

[4] M. Mohseni, N. Zobeiry, G. Fernlund. "*Experimental and numerical study of coupled gas and resin transport and its effect on porosity"*. Journal of Reinforced Plastics and Composites, Vol. 38 (23–24) 1055–1066, 2019

[5] A. R. A. Arafath, G. Fernlund, A. Poursartip. "*Gas transport in prepregs: Model and permeability experiments"*. 17th Int. Conf. Compos. Mater, 2009

[6] G. Fernlund, J. Wells, L. Farhang, J. Kay, A. Poursartip. "*Causes and remedies for porosity in composite manufacturing"*. IOP Conf. Series: Materials Science and Engineering 139, 2016

[7] James Kay, "*Gas Transport and Void Evolution in Composite Prepregs"*. PhD Thesis, The University of British Columbia, 2017

[8] R. Dave, J. L. Kardos, M. P. Dudukovic. "*A Model for Resin Flow During Composite Processing Part 2: Numerical Analysis for Unidirectional Graphite/ Epoxy Laminates"*. Polymer Composites, Vol 8, No. 2, 1987

[9] R. Dave, J. L. Kardos, M. P. Dudukovic. "*A Model for Resin Flow During Composite Processing: Part 1 -General Mathematical Development"*. Polymer Composites, Vol 8, No. 1, 1987

[10] L. E. Scriven. "*On the dynamics of phase growth"*. Chemical Engineering Science, Vol. 10 (1/2), 1959

[11] M. C. Weinberg, P. I. K. Onorato, D. R. Uhlmann. "*Behavior of Bubbles in Glassmelts: 11, Dissolution of a Stationary Bubble Containing a Diffusing and a Nondiffusing Gas"*. Journal of The American Ceramic Society, Vol. 63 (7-8) 435-438, 1980

[12] M. Amon, C. D. Denson, "*A Study of the Dynamics of Foam Growth: Analysis of the Growth of Closely Spaced Spherical Bubbles"*. Polymer Engineering and Science, Vol. 24, No. 13, 1984

[13] J. L. Kardos, M. P. Dudukovic, R. Dave. "*Void Growth and Resin Transport During Processing of Thermosetting -- Matrix Composites"*. Advances in Polymer Science, Vol. 80, 1986

[14] J. R. Wood, M. G. Bader. "*Void control for polymer-matrix composites (1): theoretical and experimental methods for determining the growth and collapse of gas bubbles"*. Composites Manufacturing, Vol. 5, No. 3, 1994

[15] M. Mohseni, N. Zobeiry, G. Fernlund. "*Process-induced matrix defects: Post-gelation"*. Composites Part A, Vol. 137, 2020

[16] Y. Ledru, G. Bernhart, R. Piquet, F. Schmidt, L. Michel. "*Coupled visco-mechanical and diffusion void growth modelling during composite curing"*. Composites Science and Technology, Vol. 70, 2139-2145, 2010

[17] T. Centea, P. Hubert. "*Modelling the effect of material properties and process parameters on tow impregnation in out-of-autoclave prepregs"*. Composites: Part A, Vol 43, 1505-1513, 2012

[18] T. S. Lundstrom. "*Bubble Transport Through Constricted Capillary Tubes With Application to Resin Transfer Molding"*. Polymer Composites, Vol 17, No. 6, 1996

[19] P. Hubert, A. Poursartip. "*A Review of Flow and Compaction Modeling Relevant to Thermoset Matrix Laminate Processing"*. Journal of Reinforced Plastics and Composites, Vol 17, No. 4, 1998

[20] C. H. Park, W. I. Lee. "*Modeling void formation and unsaturated flow in liquid composite molding processes: a survey and review"*. Journal of Reinforced Plastics and Composites, Vol 30(11) 957-977, 2011

[21] T. Centea, L. K. Grunenfelder, S. R. Nutt. "*A review of out-of-autoclave prepregs – Material properties, process phenomena, and manufacturing considerations"*. Composites: Part A, Vol 70, 132-154, 2015

[22] W. Hu, L. K. Grunenfelder, T. Centea, S. Nutt. "*In situ monitoring and analysis of void evolution in unidirectional prepreg"*. Journal of Composite Materials, Vol. 52 (21) 2847–2858, 2018

[23] W. Hu, T. Centea, S. Nutt. "*Mechanisms of inter-ply void formation during vacuum bag-only cure of woven prepregs"*. Polymer Composites, Vol. 41, 1785–1795, 2020

[24] ASTM International, ASTM E104-20a: *Standard Practice for Maintaining Constant Relative Humidity by Means of Aqueous Solutions*, ASTM International, West Conshohocken, PA, USA, 2020